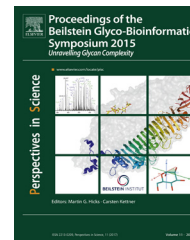




Available online at [www.sciencedirect.com](http://www.sciencedirect.com)

ScienceDirect

journal homepage: [www.elsevier.com/pisc](http://www.elsevier.com/pisc)



# FOOT: a new experiment to measure nuclear fragmentation at intermediate energies<sup>☆</sup>

S.M. Valle<sup>c,\*</sup>, A. Alexandrov<sup>a,s,ab,ac</sup>, G. Ambrosi<sup>j</sup>, S. Argirò<sup>b,m</sup>, G. Battistoni<sup>c</sup>, N. Belcari<sup>d,t</sup>, S. Biondi<sup>e,u</sup>, M.G. Bisogni<sup>d,t</sup>, G. Bruni<sup>e</sup>, S. Brambilla<sup>c</sup>, N. Camarlinghi<sup>d,t</sup>, P. Cerello<sup>b</sup>, E. Ciarrocchi<sup>d,t</sup>, A. Clozza<sup>f</sup>, G. De Lellis<sup>a,s</sup>, A. Di Crescenzo<sup>a,s</sup>, M. Durante<sup>y,ad</sup>, M. Emde<sup>aa</sup>, R. Faccini<sup>h,o</sup>, V. Ferrero<sup>b,m</sup>, F. Ferroni<sup>h,o</sup>, C. Finck<sup>x</sup>, M. Francesconi<sup>d,t</sup>, M. Franchini<sup>e,u</sup>, L. Galli<sup>d</sup>, M. Garbini<sup>e,u,l</sup>, G. Giraudò<sup>b</sup>, R. Hetzel<sup>aa</sup>, E. Iarocci<sup>f</sup>, M. Ionica<sup>j</sup>, K. Kanxheri<sup>j</sup>, A. Lauria<sup>a,s</sup>, C. La Tessa<sup>g,q</sup>, M. Marafini<sup>l,h</sup>, I. Mattei<sup>c</sup>, R. Mirabelli<sup>h,o,l</sup>, M.C. Montesi<sup>a,s</sup>, M.C. Morone<sup>i,r</sup>, M. Morrocchi<sup>d,t</sup>, S. Muraro<sup>d</sup>, L. Narici<sup>i,r</sup>, A. Pastore<sup>k</sup>, N. Pastrone<sup>b</sup>, V. Patera<sup>h,ae,l</sup>, M. Pullia<sup>z</sup>, L. Ramello<sup>b,n</sup>, V. Rosso<sup>d,t</sup>, M. Rovituso<sup>g</sup>, C. Sanelli<sup>f</sup>, A. Sarti<sup>ae,f,l</sup>, G. Sartorelli<sup>e,u</sup>, O. Sato<sup>p</sup>, A. Schiavi<sup>h,ae</sup>, C. Schuy<sup>y</sup>, E. Scifoni<sup>g</sup>, A. Sciubba<sup>ae,h,l</sup>, M. Selvi<sup>e</sup>, L. Servoli<sup>j</sup>, M. Sitta<sup>b,n</sup>, R. Spighi<sup>e</sup>, E. Spiriti<sup>f</sup>, G. Sportelli<sup>d,t</sup>, A. Stahl<sup>aa</sup>, F. Tommasino<sup>g,q</sup>, G. Traini<sup>o,h,l</sup>, M. Vanstalle<sup>x</sup>, M. Villa<sup>e,u</sup>, U. Weber<sup>y</sup>, A. Zoccoli<sup>e,u</sup>

<sup>a</sup> Istituto Nazionale di Fisica Nucleare (INFN), Sezione di Napoli, Napoli, Italy

<sup>b</sup> Istituto Nazionale di Fisica Nucleare (INFN), Sezione di Torino, Torino, Italy

<sup>c</sup> Istituto Nazionale di Fisica Nucleare (INFN), Sezione di Milano, Milano, Italy

<sup>d</sup> Istituto Nazionale di Fisica Nucleare (INFN), Sezione di Pisa, Pisa, Italy

<sup>e</sup> Istituto Nazionale di Fisica Nucleare (INFN), Sezione di Bologna, Bologna, Italy

<sup>f</sup> Istituto Nazionale di Fisica Nucleare (INFN), Laboratori Nazionali di Frascati, Frascati, Italy

<sup>g</sup> Trento Institute for Fundamental Physics and Applications, Istituto Nazionale di Fisica Nucleare (TIFPA-INFN), Trento, Italy

Available online 2 July 2019

<sup>☆</sup> This article is part of a special issue 27th-ICNTRM.

\* Corresponding author.

E-mail address: [serena.valle@mi.infn.it](mailto:serena.valle@mi.infn.it) (S.M. Valle).

<https://doi.org/10.1016/j.pisc.2019.100415>

2213-0209/© 2019 Published by Elsevier GmbH. This is an open access article under the CC BY-NC-ND license (<http://creativecommons.org/licenses/by-nc-nd/4.0/>).

- <sup>h</sup> Istituto Nazionale di Fisica Nucleare (INFN), Sezione di Roma 1, Roma, Italy  
<sup>i</sup> Istituto Nazionale di Fisica Nucleare (INFN), Sezione di Roma 2, Roma, Italy  
<sup>j</sup> Istituto Nazionale di Fisica Nucleare (INFN), Sezione di Perugia, Perugia, Italy  
<sup>k</sup> Istituto Nazionale di Fisica Nucleare (INFN), Sezione di Bari, Bari, Italy  
<sup>l</sup> Museo Storico della Fisica e Centro Studi e Ricerche Enrico Fermi, Roma, Italy  
<sup>m</sup> Università di Torino, Department of Physics, Torino, Italy  
<sup>n</sup> Università del Piemonte Orientale, Department of Science and Technological Innovation, Alessandria, Italy  
<sup>o</sup> Università di Roma "La Sapienza", Department of Physics, Roma, Italy  
<sup>p</sup> Nagoya University, Department of Physics, Nagoya, Japan  
<sup>q</sup> Università di Trento, Department of Physics, Trento, Italy  
<sup>r</sup> Università di Roma "Tor Vergata", Department of Physics, Roma, Italy  
<sup>s</sup> Università di Napoli "Federico II", Department of Physics, Napoli, Italy  
<sup>t</sup> Università di Pisa, Department of Physics, Pisa, Italy  
<sup>u</sup> Università di Bologna, Department of Physics and Astronomy, Bologna, Italy  
<sup>x</sup> Université de Strasbourg, CNRS, IPHC UMR 7871, Strasbourg F-67000, France  
<sup>y</sup> GSI Helmholtzzentrum für Schwerionenforschung, Biophysics Department, Darmstadt, Germany  
<sup>z</sup> Centro Nazionale di Adroterapia Oncologica (CNAO), Italy  
<sup>aa</sup> RWTH Aachen University, Physics Institute III B, Aachen, Germany  
<sup>ab</sup> National University of Science and Technology MISIS, RUS-119049, Russia  
<sup>ac</sup> Lebedev Physical Institute of the Russian Academy of Sciences, Moscow RUS-119991, Russia  
<sup>ad</sup> Technische Universität Darmstadt Institut für Festkörperphysik, Darmstadt, Germany  
<sup>ae</sup> Università di Roma "La Sapienza", Scienze di Base e Applicate per l'Ingegneria Department (SBAI), Roma, Italy

## KEYWORDS

Hadrontherapy;  
 Nuclear fragmentation  
 cross sections;  
 Tracking detectors;  
 Scintillating detectors

**Summary:** Charged particle therapy exploits proton or  $^{12}\text{C}$  beams to treat deep-seated solid tumors. Due to the advantageous characteristics of charged particles energy deposition in matter, the maximum of the dose is released to the tumor at the end of the beam range, in the Bragg peak region. However, the beam nuclear interactions with the patient tissues induces fragmentation both of projectile and target nuclei and needs to be carefully taken into account. In proton treatments, target fragmentation produces low energy, short range fragments along all the beam range, which deposit a non negligible dose in the entry channel. In  $^{12}\text{C}$  treatments the main concern is represented by long range fragments due to beam fragmentation that release their dose in the healthy tissues beyond the tumor. The FOOT experiment (FragmentatiOn Of Target) of INFN is designed to study these processes, in order to improve the nuclear fragmentation description in next generation Treatment Planning Systems and the treatment plans quality. Target ( $^{16}\text{O}$  and  $^{12}\text{C}$  nuclei) fragmentation induced by  $^{-}$ proton beams at therapeutic energies will be studied via an inverse kinematic approach, where  $^{16}\text{O}$  and  $^{12}\text{C}$  therapeutic beams impinge on graphite and hydrocarbon targets to provide the nuclear fragmentation cross section on hydrogen. Projectile fragmentation of  $^{16}\text{O}$  and  $^{12}\text{C}$  beams will be explored as well. The FOOT detector includes a magnetic spectrometer for the fragments momentum measurement, a plastic scintillator for  $\Delta E$  and time of flight measurements and a crystal calorimeter to measure the fragments kinetic energy. These measurements will be combined in order to make an accurate fragment charge and isotopic identification.

© 2019 Published by Elsevier GmbH. This is an open access article under the CC BY-NC-ND license (<http://creativecommons.org/licenses/by-nc-nd/4.0/>).

## Introduction

Charged Particle Therapy (CPT) is a widespread technique to treat deep-seated solid tumors. The advantageous depth-dose deposition profile characteristic of charged hadrons allows to precisely fit the dose release to the tumor volume, while efficiently sparing the healthy tissues surrounding the tumor. In addition, CPT is highly recommended in case of radioresistant tumors because of the high Relative Biological Effectiveness (RBE) of charged hadrons, particularly in case of heavy ions such as Carbon and Oxygen.

Clinically, proton RBE is conventionally set to a constant value of 1.1 despite of the experimentally demonstrated RBE variations, which depend on both physical and biological parameters. It has been hypothesized that an increase of the proton RBE can be induced by the nuclear reactions of the beam with the patient tissues (Tommasino and Durante, 2015): in inelastic interactions, in fact, several low energy and high Z fragments can be produced. Target fragments

have in fact significantly higher RBE values with respect to protons.

In case of  $Z > 1$  ion beam therapy, nuclear fragmentation is also responsible for the production projectile fragments, which have a lower charge and mass, and consequently they travel farther than the primary beam and produce a dose tail beyond the Bragg peak position.

Experimental data on beam fragmentation (mainly  $^{16}\text{O}$  and  $^{12}\text{C}$ ) are scarce, while measurements of the target fragmentation due to p-nucleus interactions are missing. However, since the fragments contribution to the overall released dose can be significant, a new study of their production cross sections is strongly needed to take their contribution into account during the treatment planning stage.

The goal of the FOOT (FragmentatiOn Of Target) experiment (Patera et al., 2017) of INFN (Istituto Nazionale di Fisica Nucleare) is to estimate both target and beam fragmentation cross sections to provide new data for medical physicists and radiobiologists and to improve the new generation Treatment Planning Systems.

## Experiment main goals and strategies

Due to kinematic reason, heavy fragments ( $Z > 3$ ) are forward emitted within a cone of  $10^\circ$  semiaperture with respect to the beam axis, whereas light fragments are also scattered at larger angles. Hence, the FOOT apparatus has been designed with two different setups: an electronic experimental setup, aiming to study heavy fragments, and an emulsion chamber, able to measure light fragments at larger angles.

The electronic setup has been optimized to study heavy ( $Z > 3$ ) target fragment production, aiming to provide:

- different fragments production cross sections
- charge  $Z$  and mass  $A$  fragments identification
- fragment energy spectra

The measurement of the target fragmentation induced by protons is a challenging task due to the low energy and short

range ( $\sim$ tens of  $\mu\text{m}$ ) of the produced fragments. For this reason, an inverse kinematic approach will be implemented: the fragmentation of tissue-like ion beams (mainly C and O, which are the main constituents of human body) impinging on a Hydrogen enriched target will be studied. As a result, secondary fragments will have boosted energy and longer range. By applying the Lorentz transformation, it will be possible to switch from the laboratory frame to the "patient frame" (Dudouet et al., 2013). To overcome the problems concerning the construction of a pure Hydrogen target, two different targets will be employed: one made of Carbon, while the other of a hydrogenated material, such as  $\text{C}_2\text{H}_4$ . Differential cross sections on Hydrogen will be calculated by subtraction from the data obtained using a pure C target (Dudouet et al., 2013) (Fig. 1).

To calculate the cross sections and to correctly identify charge and mass of the secondary fragments, the detector will measure their momentum  $p$ , kinetic energy  $E_k$ , time of flight ( $TOF$ ) and energy release  $\Delta E$ . The charge can be in fact identified by putting together the information from  $\Delta E$  measurements with  $TOF$ , while the mass can be retrieved by  $p$ ,  $TOF$  and  $E_k$  through the following three equations:

$$p = mc\beta\gamma \quad (1)$$

$$E_k = mc^2(\gamma - 1) \quad (2)$$

$$E_k = \sqrt{p^2c^2 + m^2c^4} - mc^2 \quad (3)$$

where  $\beta$  and  $\gamma$  are obtained from the  $TOF$ .

To achieve the requested resolution on cross sections and particle identification, the main measurements performances need to be the following:

- $\sigma(p)/p \sim 5\%$
- $\sigma(E_k)/E_k \sim 2\%$
- $\sigma(\Delta E)/\Delta E \sim 3 - 10\%$
- $\sigma(TOF)/TOF \sim 100\text{ps}$

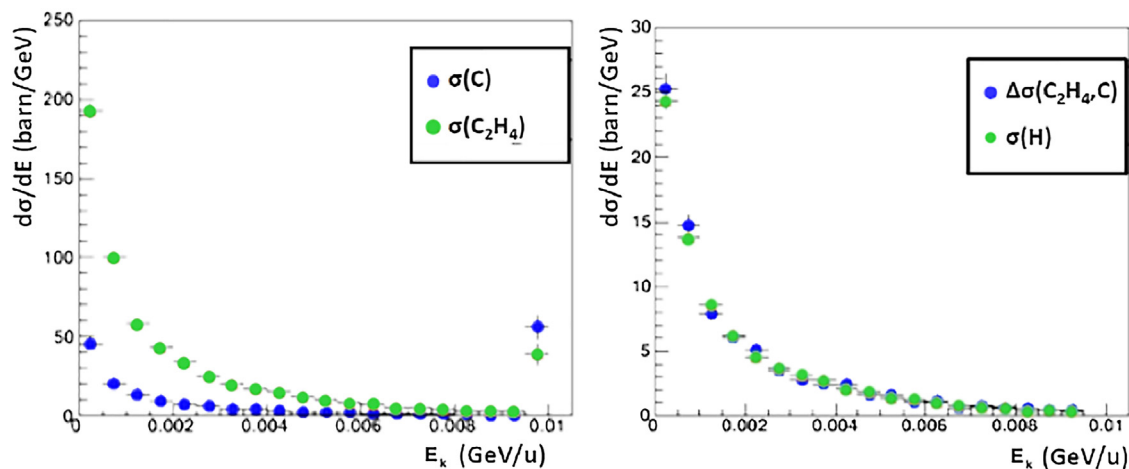


**Figure 1** Reconstruction of energy differential cross sections of C fragments in inverse kinematics for a  $^{12}\text{C}$  beam on C and  $\text{C}_2\text{H}_4$  target (left panel) and on H obtained either by subtraction or directly on H target (right panel). Data have been obtained from FLUKA simulations.

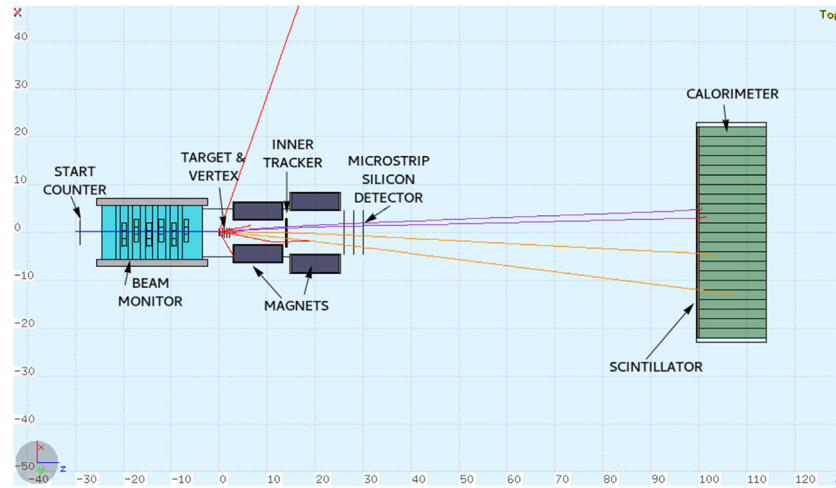


Figure 2 2D view of the detector produced with Flair, the FLUKA geoviewer.

## Electronic experimental setup

Three different regions can be identified in the project of the electronic setup (Fig. 2):

- Pre-target region. A thin plastic scintillator counter will give trigger information and the *TOF* start time, while a drift chamber will monitor the beam direction and position. The target is placed immediately downstream the drift chamber.
- Magnetic spectrometer region. Beyond the target, a telescope of Silicon pixel trackers will reconstruct the vertex position and provide the initial tracking. Then two cylindrical permanent magnets in the Halbach configuration will provide the magnetic field (maximum value  $\sim 0.8$  T). Two other layers of Silicon pixel trackers and a telescope of Silicon microstrips will be placed between and at the end of the magnets respectively. All these tracking elements will allow the measurement of fragments momentum.
- Calorimeter region. A detector made of two orthogonal planes consisting of plastic scintillator bars will measure  $\Delta E$  and *TOF*. Finally, the measurement of kinetic energy is provided by a calorimeter made of BGO crystals.

In order to optimize the detector design and to study its expected performances, Monte Carlo simulations have been built using the FLUKA code (Ferrari et al., 2005; Böhlen et al., 2014).

## Expected performances

A preliminary study of the detector performances on charge and mass resolutions has been performed on the basis of the FLUKA simulated data. The *Z* values, simply retrieved from the energy released in the plastic scintillator, are presented along with their resolutions in Table 1 for some selected fragments ( $^1\text{H}$ ,  $^4\text{He}$ ,  $^7\text{Li}$ ,  $^9\text{Be}$ ,  $^{11}\text{B}$ ,  $^{12}\text{C}$  and  $^{14}\text{N}$ ); these values were obtained applying a  $\Delta E$  resolution parametrized as a function on the deposited energy and limited to the range 3–10%.

Having the possibility to determine at the same time  $E_k$ , *TOF* and *p* for each fragment, it is possible to reconstruct its mass by coupling the measured quantities in three different correlated ways: as an example, in the left panel of Fig. 3 it is reported the Nitrogen mass coupling the information from  $E_k$  and *TOF* with the above mentioned resolutions. To improve the resolution, a global fit obtained with the Augmented Lagrangian Method (ALM) (Hestenes, 1969) with the mass obtained in all the three ways as constraints has been applied (Fig. 3 right).

The achievable resolutions on mass determination for the selected fragments are reported in Table 2.

## Other goals of FOOT experiment

An emulsion cloud chamber will provide complementary light fragments ( $Z \leq 3$ ) measurements (De Lellis et al., 2011) (Fig. 4). It will provide measurements of fragments emitted up to  $70^\circ$  (mainly protons, deuterons, tritons, Helium and Lithium ions). In this case, the pre-target region of the electronic setup will monitor the incoming primary

Table 1 True and reconstructed *Z* values of the selected fragments, obtained from a FLUKA simulation of the detector.

| Frag.                   | $^7\text{Li}$   | $^9\text{Be}$   | $^{11}\text{B}$ | $^{12}\text{C}$ | $^{14}\text{N}$ |
|-------------------------|-----------------|-----------------|-----------------|-----------------|-----------------|
| <i>Z</i>                | 3               | 4               | 5               | 6               | 7               |
| <i>Z</i> <sub>rec</sub> | $3.02 \pm 0.08$ | $4.05 \pm 0.10$ | $5.06 \pm 0.12$ | $6.08 \pm 0.14$ | $7.11 \pm 0.16$ |

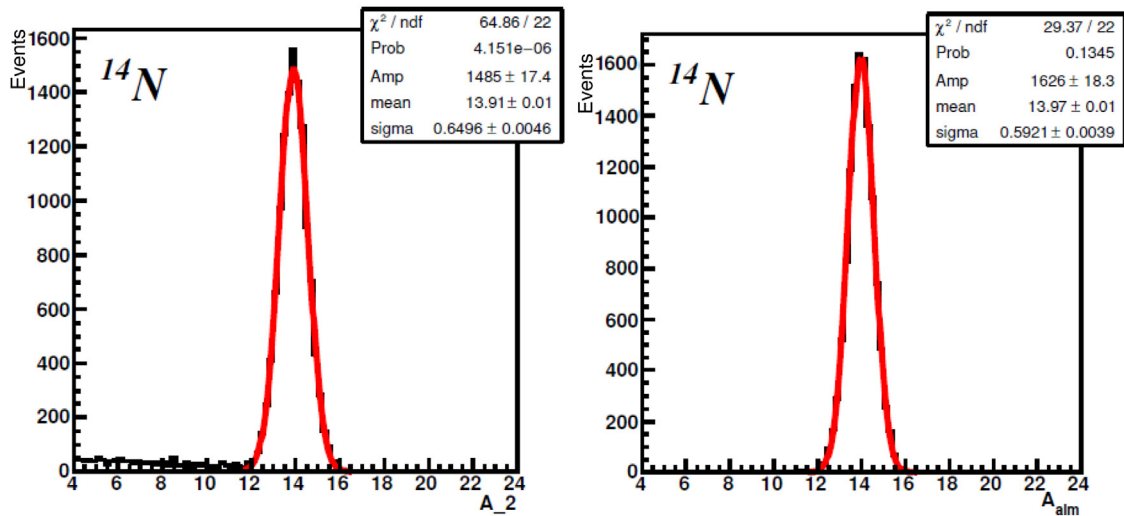


Figure 3 Example of  $^{14}\text{N}$  mass determined from the kinetic energy and  $TOF$  measurements (left panel) and determined by coupling all the information from  $E_k$ ,  $TOF$  and  $p$  and by applying both a  $\chi^2$  cut and the ALM.

Table 2 True and reconstructed  $A$  values of the selected fragments, obtained from a FLUKA simulation of the detector.

| Frag.            | $^7\text{Li}$   | $^9\text{Be}$   | $^{11}\text{B}$  | $^{12}\text{C}$  | $^{14}\text{N}$  |
|------------------|-----------------|-----------------|------------------|------------------|------------------|
| $A$              | 7               | 9               | 11               | 12               | 14               |
| $A_{\text{rec}}$ | $7.02 \pm 0.32$ | $9.01 \pm 0.40$ | $11.01 \pm 0.50$ | $11.98 \pm 0.52$ | $13.98 \pm 0.59$ |

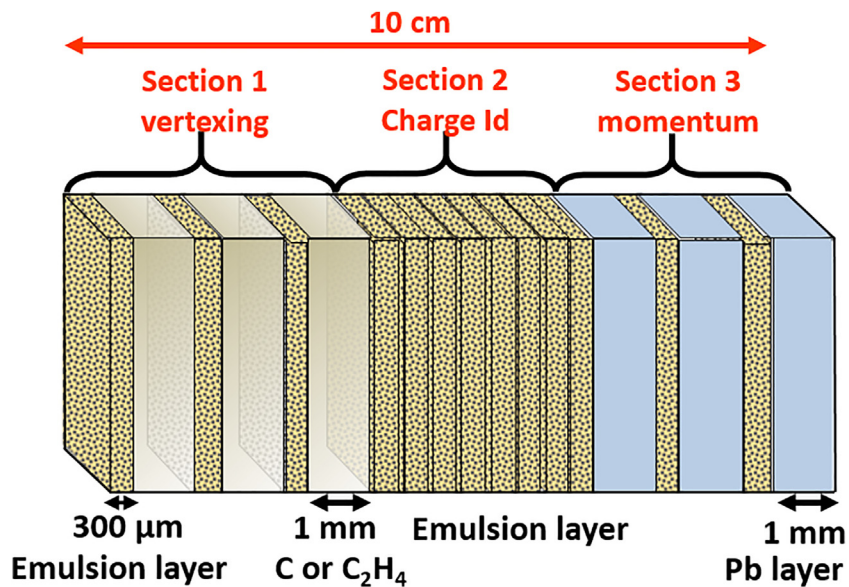


Figure 4 Scheme of the emulsion spectrometer detector.

beam, while the emulsion chamber will act as both target and fragments detector: the first section, where target layers (C or  $\text{C}_2\text{H}_4$ ) are alternated with emulsion films will reconstruct the interaction vertex; the second one, composed of emulsion films will reconstruct the charge; the last one, in which the emulsion films are interleaved with Lead layers, will measure fragments energy and momentum.

In addition, data that will be acquired by means of the electronic setup will be studied also in direct kinematics to estimate projectile fragmentation cross sections, which are required to improve nuclear reactions description in Treatment Planning Systems.

Along with the study of cross sections relevant in CPT, also the fragmentation induced by higher energy beams will be investigated to provide data for space radioprotection.

## Conclusion

The FOOT goal is to experimentally measure target fragmentation cross sections, aiming to improve the protontherapy treatment quality. An inverse kinematics strategy will be adopted to study target fragmentation and two experimental setups are at present under development. FLUKA simulations are currently employed for optimization and performances studies. Along with target fragmentation, FOOT will also study projectile cross sections which are of great interest in heavy ion therapy. Moreover, by considering the operation of FOOT at higher energies, useful results for the development of radioprotection for long duration and far from earth space missions could be achieved.

## Acknowledgments

We wish to thank the INFN Scientific Commission 3 (CSN3) for funding the participation to the conference ICNTRM 2017.

## References

- Böhlen, T.T., et al., 2014. The FLUKA code: developments and challenges for high energy and medical applications. *Nucl. Data Sheets* 120, 211–214.
- De Lellis, G., et al., 2011. [Nuclear emulsions](#). In: [Fabjan, C.W., Schopper, H. \(Eds.\), Elementary Particles: Detectors for Particles and Radiation](#), vol. 21B. Springer.
- Dudouet, J., et al., 2013. [Double-differential fragmentation cross-section measurements of 95 MeV/nucleon  \$^{12}\text{C}\$  beams on thin targets for hadron therapy](#). *Phys. Rev. C* 88 (2), 024606.
- Ferrari, A., et al., 2005. [FLUKA: A Multi-Particle Transport Code](#). INFN-TC-05-11, CERN 2005-10, SLAC-R-773L.
- Hestenes, M.R., 1969. [Multiplier and gradient methods](#). *J. Optim. Theory Appl.* 4 (5), 303–320.
- Patera, V., et al., 2017. [The Foot \(Fragmentation Of Target\) Experiment](#). *PoS 128. ISO 690*.
- Tommasino, F., Durante, M., 2015. [Proton radiobiology](#). *Cancers* 7 (1), 353–381.